Synthesis and Photochemical Properties of Manganese(I) Tricarbonyl Diimine Complexes Bound to Tetrazolato Ligands

Synthesis and photochemical properties of Mn(I) tricarbonyl diimine complexes bound to tetrazolato ligands

Synthesis and photochemical properties of Mn(I) tricarbonyl diimine complexes bound to tetrazolato ligands

Matthew J. Stout,[a] Alessandra Stefan,[b,c] Brian W. Skelton,[d] Alexandre N. Sobolev,[d] Massimiliano Massi,*[a] Alejandro Hochkoeppler [b,c], Stefano Stagni,[e] Peter V. Simpson*[a]

Abstract: Ten manganese(I) tricarbonyl diimine complexes bound to variably functionalised 5-aryl-tetrazolato ligands were prepared, and their photochemical properties were investigated. Upon exposure to light at 365 nm, each complex decomposed to its free diimine and tetrazolato ligands, simultaneously dissociating three CO ligands, as evidenced by changes in the IR spectra of the irradiated complexes over time. The anti-bacterial properties of one of these complexes were tested against *Escherichia coli*. While the complex displayed no effect on the bacterial growth in the dark, pre-irradiated solutions inhibited bacterial growth. Comparative studies revealed that the antibacterial properties originate from the presence of free 1,10-phenanthroline.

Introduction

Carbon monoxide is a very important signalling molecule within complex organisms. It is endogenously produced at low concentrations following the breakdown of free haemoglobin by the enzyme family haem oxygenases (HOs), as a response to tissue damage.[1-4] Consequently, many studies have been conducted on the therapeutic properties of administered exogenous CO, demonstrating beneficial effects such as anti-inflammation, tissue protection, anti-cancer, and anti-bacterial.[5-10] However, due to the high toxicity of CO and lack of spatial specificity, administering CO as an inhaled gas presents some significant drawbacks.[11] Early research in this field by Motterlini and co-workers[12] addressed this problem by preparing the very first carbon monoxide releasing molecules (CORMs) to release CO endogenously within the body, including the first photoactivated CORM (photoCORM), dimanganese decacarbonyl (referred to as CORM-1). CORM-1 was the first evidence that a transition metal carbonyl complex could potentially act as a carrier to deliver CO. However, it lacked solubility in aqueous media, was highly toxic and required harmful UV light for activation.[13-14] Since this early research, the field has rapidly expanded with photoCORMs designed for high solubility in biological media, tissue specificity, defined CO release rate, and red-shifted light absorption.[15-26] Previous research within our group explored the use of luminescent rhenium complexes of the type Re(N^N)(CO)$_3$L, where N^N is a diimine-type ligand such as 1,10-phenathroline and L is a functionalized 5-aryltetrazolato ligand, as cellular probes.[27-30] Our studies indicated that this class of complexes possessed suitable properties as building blocks for the preparation of cellular markers with specifically tailored properties, as for example the staining of polar lipids in live cells and tissues. The cytotoxicity of these complexes was quite low, which was ascribed to their inertness towards potential ligand exchange reactions in cells. On the other hand, manganese complexes bound to tetrazolate anions are relatively unexplored, and virtually none of these species has been investigated for biological applications.[31-34] We therefore envisaged that the corresponding manganese analogues of our previously published rhenium complexes could possess CO-releasing properties and tuning of the biological properties such as organelle targeting.

In this work, we present the synthesis, structural and photochemical characterization of ten neutral complexes of the type Mn(N^N)(CO)$_3$L. Their photochemical properties have been assessed by a combination of UV-Vis, IR and NMR spectroscopies, revealing decomposition of the species with the simultaneous liberation of three CO ligands. This feature was preliminarily explored to assess inhibition of *Escherichia coli* bacterial growth.

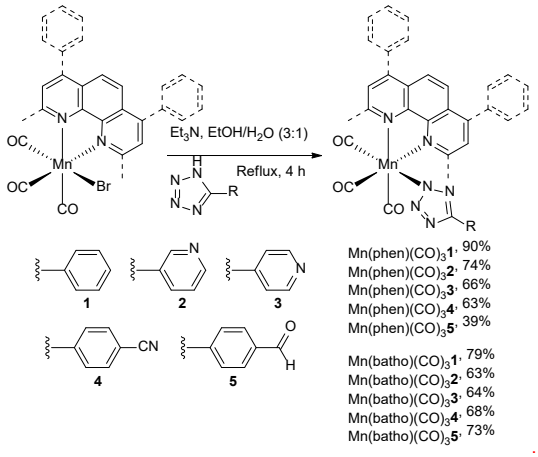

Scheme 1. Synthesis of manganese tetrazolate complexes.

Results and Discussion

The preparation of the precursor complexes Mn(phen)(CO)$_3$Br and Mn(batho)(CO)$_3$Br (where phen is 1,10-phenanthroline and batho is bathocuproine), as well as their subsequent reactions with tetrazoles (**1**-**5**H), were based on a modification of previously published works (Scheme 1).[35-37] The Mn(phen)(CO)$_3$Br and Mn(batho)(CO)$_3$Br precursors were heated at reflux in the dark with a slight excess of the corresponding tetrazole and triethylamine in a 3:1 ethanol/water mixture. All the complexes were purified following by filtration and subsequent re-precipitation, and were obtained as yellow powders in moderate to high yields. The complexes are soluble in all common organic solvents including acetone, dichloromethane, methanol, acetonitrile, dimethylformamide, and dimethylsulfoxide.

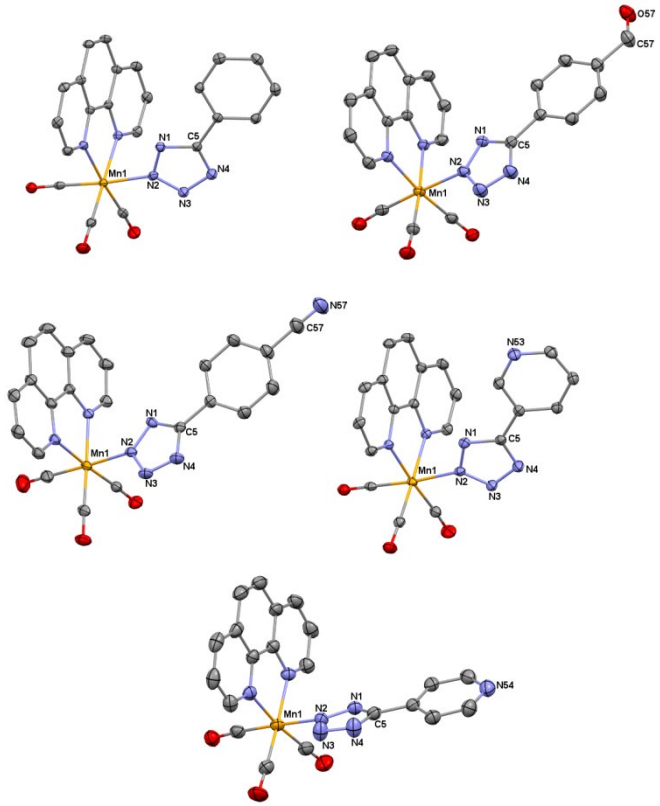

Figure 1. X-ray crystal structures of Mn(phen)$(CO)_3$(**1-5**) with displacement ellipsoids drawn at the 50% probability level. Hydrogen atoms have been omitted for clarity.

The IR spectra of all complexes contained two CO bands, with the lower energy band being the superimposition of two quasi-degenerate peaks, consistently with three carbonyl ligands in a *facial* arrangement. The frequencies of the CO stretching vibrations were very similar for all the complexes, yet all of them showed an increase in value compared to the starting bromo complex. The increase in CO frequency was rationalized by a slight decrease in electron density on passing from the bromo to the tetrazolato ligands. The ^{1}H and ^{13}C NMR spectra of the complexes exhibited the expected number of signals, highlighting the symmetric arrangement of the phen and batho ligands originating from the *facial* configuration of the carbonyl ligands. Further investigation of the complexes by ^{13}C-NMR showed signals between 160–164 ppm for the quaternary carbon of the various tetrazole rings, indicative of the coordination of the Mn fragment to the N2 atom.[35-37]

The single crystal X-ray diffraction structures of complexes Mn(phen)$(CO)_3$(**1-5**) revealed similar structures (Figure 1), where in all cases the Mn centres display a slightly distorted octahedral geometry with three CO ligands bound in a *facial* arrangement. All the tetrazole ligands are bound through their N2 position in a similar manner to the previously reported rhenium complexes. After several attempts, the corresponding analogous batho complexes could not be crystallized.

The absorption spectra of all complexes recorded from diluted dichloromethane solutions (see Figure 2 for two examples displaying the phen and batho complexes bound to **4**; the remaining absorption spectra are available in the SI) exhibit high energy bands in the 250-350 nm region**,** and broad featureless bands with lower molar absorptivity between 350 and 500 nm. The high energy bands are attributed to ligand-centred (LC) π-π^* transitions within the phen and batho ligands. On the other hand, the red-shifted broad bands are typical of metal-to-ligand charge transfer (MLCT) transitions from the manganese centre to the phen and batho ligands. The MLCT absorption maxima of the complexes appear in the 350-370 nm region and are blue shifted by around ~60 nm when compared to the starting material complexes Mn(phen)$(CO)_3$Br and Mn(batho)$(CO)_3$Br (~430 nm).[38] No significant shift in MLCT absorption maxima was observed between the Mn(phen)$(CO)_3$(**1-5**) and Mn(Batho)$(CO)_3$(**1-5**) complexes.

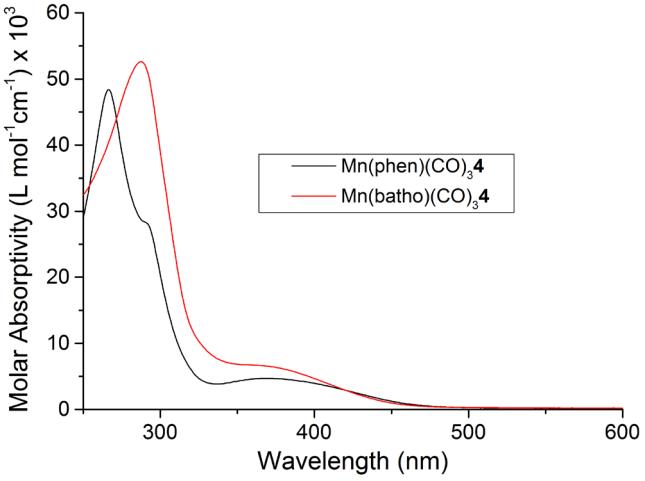

Figure 2. UV-VIS spectra of Mn(phen/batho)$(CO)_3$**4** from diluted dichloromethane solutions.

When stored in the dark, either in the solid state or in solution (acetone and dichloromethane), the complexes appear to be stable, as verified by the lack of changes in their IR and NMR spectra over time. When exposed to standard ambient illumination within the laboratory, however, the complexes in the solid state changed color from pale yellow to a mixture of white and brown within a day. This color change occurred significantly faster when the complexes were dissolved, forming a colorless solution containing a brown precipitate within hours. In order to investigate the photoreaction occurring when the complexes are exposed to light, photolysis experiments were performed by irradiating dichloromethane or acetone solutions containing the complexes with a 365 nm pen lamp source. The irradiated solutions were then monitored by IR spectroscopy to highlight changes in the carbonyl bands. The simultaneous disappearance of all three CO stretches upon illumination was observed within 25 minutes for all complexes. Using complex Mn(phen)$(CO)_3$**4** as an example, the presence of CO peaks

2036 and 1942 cm^{-1} completely collapsed after 25 minutes of photolysis (Figure 3; see SI for the remaining complexes) indicating that no Mn-CO bonds remained. During this transition, the solution went from yellow (0 min) to dark orange (4-16 min), then eventually becoming clear and colorless with the concomitant formation of a dark precipitate (25 min). The absence of visible color suggests that Mn was no longer bound to phen. During photolysis, the formation of minor sharp bands with weak intensity was observed, tentatively attributed to short-lived intermediate manganese species forming and decomposing during the photolysis, although these intermediates were not completely characterized. The photolysis experiment gave analogous results when the starting solution was degassed to remove dissolved O_2.

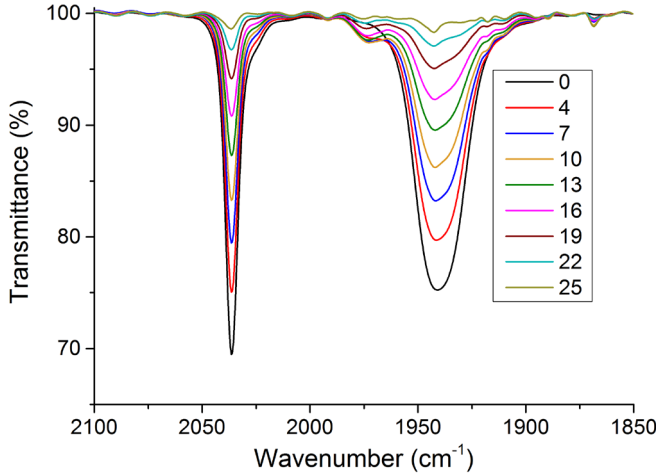

Figure 3. Progressive IR spectra (carbonyl bands region) of a dichloromethane containing the complex Mn(phen)$(CO)_3$**4** irradiated with a 365 nm pen lamp source. The time intervals presented in the framed legend are expressed in minutes.

A fully photolyzed solution of Mn(phen)$(CO)_3$**4** was analyzed using ^{1}H-NMR to determine the identity of the formed species. Initially, a broad and unresolvable band was observed in the aromatic region of the spectra. It was postulated that Mn(I) had oxidised to a paramagnetic Mn species that caused significant line broadening in the ^{1}H-NMR spectrum. Pre-filtration of the photolyzed solution produced a spectrum with better defined peaks, albeit still broad in appearance (Figure 4). These broad peaks were directly compared with the spectra of the free phen and the triethylammonium salt of **4**$^-$. The signals at 9.11, 8.50, 8.00 and 7.78 ppm matched for free phen, whilst the signals at 8.14 and 7.82 ppm fit with the deprotonated tetrazole ligand.

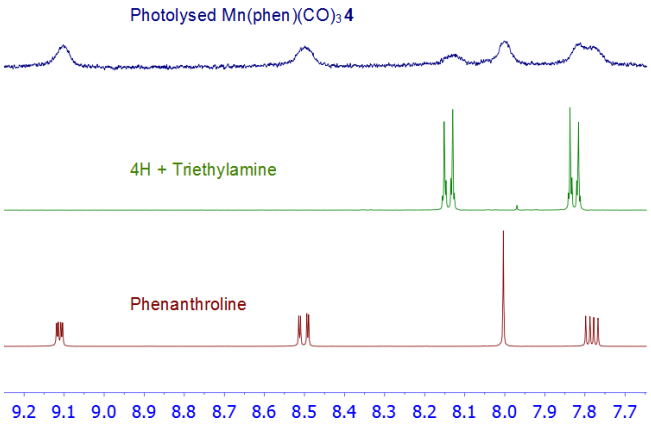

Figure 4. Stacked DMSO-d_6 H-NMR spectra: Photolyzed solution of Mn(phen)$(CO)_3$**4** (blue), free 4H and triethylamine (green), free phenanthroline (red).

In order to determine the identity of the excited state where decomposition of the complexes occurs, dichloromethane solutions of Mn(phen)$(CO)_3$**4** and Mn(batho)$(CO)_3$**4**, used as exemplar for phen and batho containing manganese complexes, were exposed to a range of wavelengths from purple (415 nm) to yellow (555 nm), using a PoliLight FL 500 (Universal Forensic Light) as the source. Figure 5 displays the decrease of intensity of the A'_1 carbonyl band upon irradiation with various wavelengths, normalised to the intensity of the carbonyl band from a solution maintained in the dark (as a ratio of transmittance from photolysed solution, T, and transmittance of solution kept in the dark, T_i). The extent of photolysis rapidly decreases when the wavelengths elongate past 490 nm, suggesting that the complexes decompose from MLCT excited states.

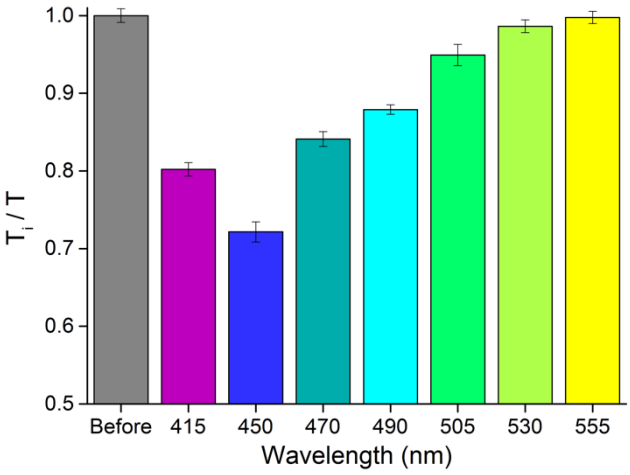

Figure 5. Ratio of initial transmittance (T_i) over post photolysis transmittance (T) for the Mn(phen)$(CO)_3$**4** carbonyl (A'$_1$). CO release at different wavelengths of irradiation using PoliLight FL 500. The error bars correspond to the standard deviation of three independent measurements.

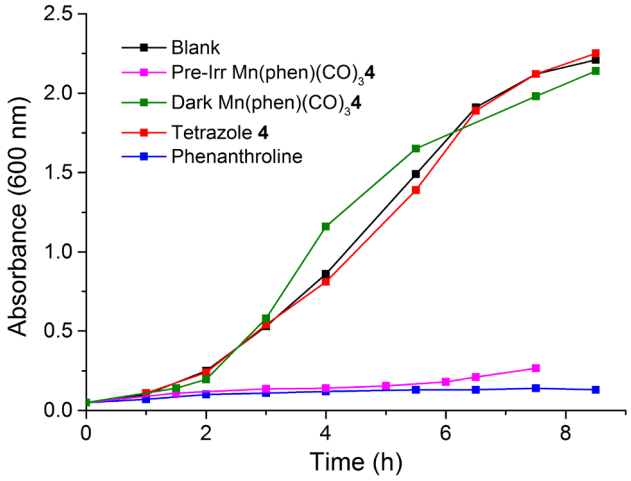

Figure 6. *E. coli* growth curves at 37 °C in the presence of 100 μM Mn(phen)$(CO)_3$**4** pre-photolysed or maintained in the dark (pink and green lines, respectively), phenanthroline (blue line) and tetrazole **4** (red line). A control culture containing DMSO alone (1.2%) was prepared (dark line).

Mn(phen)$(CO)_3$**4** was tested for its antibacterial activity against Gram-negative *E. coli*, as photoCORMs have recently been found to be very efficient anti-bacterial agents.[39-44] A comparative experiment was set up to individually investigate an aqueous solution (1.2% DMSO in H_2O, pH 6.9) of the intact complex (maintained in the dark) and a prefiltered (to remove unknown manganese oxide species), photolyzed solution (pre-irradiated with 365 nm until the UV-Vis spectrum did not show any MLCT band). The growth curves obtained were also compared with a blank (1.2% DMSO/LB only) and with aqueous solutions containing only the tetrazole or the phenanthroline ligand, all at a concentration of 100 μM. The resulting growth curves are shown in Figure 6. The results indicate that while the intact complex does not inhibit *E. coli* growth, the photolysed solution has a strong inhibitory effect with a fully suppression of the bacterial growth. When Mn(phen)$(CO)_3$**4** was pre-photolyzed, *E. coli* growth was completely inhibited at 100 μM sample concentration, whilst a 5 μM concentration did not significantly alter the growth rate of *E. coli* (see SI). Subsequent growth curves conducted on free ligands confirmed that tetrazole **4** had no effect on *E. coli* growth at any concentrations tested, whilst phenanthroline completely inhibited bacterial growth similarly to the pre-irradited Mn(phen)$(CO)_3$**4** at 100 μM concentration and slightly decreased the rate of bacterial growth when used at 5 μM. This result is in agreement with previous research showing antibacterial properties of phen.[45]

Conclusions

A series of ten manganese(I) complexes were synthesised and fully characterised, including X-ray crystal structure analysis for the five complexes bound to the phenanthroline. All compounds are stable in the dark. However, upon excitation to the lowest MLCT manifold, all three carbonyls are lost simultaneously, leading to the release of phen/batho and corresponding tetrazolato ligands. The complexes could be activated with a variety of light source from low power artificial lab light to a high power PoliLight, ranging from wavelengths 365-555 nm. Bacterial growth inhibition was tested for solutions containing either the intact of the photolysed complex, with inhibition of *E. coli* observed for the latter. This effect seems to be caused by the presence of phen species since phenanthroline alone inhibited bacterial growth to a similar level observed in the presence of the pre-irradited Mn(phen)$(CO)_3$**4**.

Experimental Section

General considerations

All reagents and solvents were purchased from Sigma Aldrich, Alfa Aesar and Strem Chemicals and used as received without further purification. All experiments were performed in the dark by wrapping glassware in aluminium foil. Nuclear magnetic resonance spectra were recorded using a Bruker Avance 400 spectrometer (400.1 MHz for ^{1}H; 100 MHz for ^{13}C) at 300 K. All the NMR spectra were calibrated to residual solvent signals. Infrared spectra were recorded using a Perkin Elmer Spectrum 100 FT-IR spectrometer. Elemental analyses were obtained at Curtin University using a Thermo Finnigan EA 1112 Series Flash. Absorption spectra were recorded at room temperature using a Cary 4000 UV-Vis spectrometer.

Lamp photolysis experiments were carried out using a UVP Blak-Rays B-100AP High Intensity UV lamp with a 100 W bulb at a single wavelength

output of 365 nm. The experiments were performed under darkness, the complexes dissolved in dichloromethane (3 mL, *ca.* 7-8 mM) and stored in in a quartz cuvette. The distance between quartz and lamp source was kept constant at a 3 cm distance. The lamp was switched off at set intervals and the solutions analysed in a NaCl (5 mm) disc on a Perkin-Elmer Spectrum 2000 FT-IR spectrometer. The range of wavelengths able to activate the complexes were tested using a PoliLight FL 500 Universal Forensic Light. Complexes were dissolved in dichloromethane (3 mL, *ca.* 7-8 mM) and placed in a quartz cuvette and kept 6 cm away from the PoliLight. Solutions were irradiated for 15 seconds each, and CO loss was measured using a NaCl (5 mm) disc on a Perkin-Elmer Spectrum 2000 FT-IR spectrometer.

Escherichia coli TOP10 strain was streaked from a 20% glycerol stock on Luria-Bertani (LB) agar plates (10 g/L tryptone, 5 g/L yeast extract, 10 g/L NaCl, 15 g/L agar), and grown at 37°C overnight. A single colony was used to prepare the pre-culture in LB liquid medium. After overnight incubation at 37 °C under shaking (180 rpm), the pre-culture was used to inoculate independent cultures (5 mL of fresh LB) containing different concentrations of Mn(phen)$(CO)_3$**4** dissolved in dimethylsulfoxide/water (50:50). A control culture in absence of any complex containing DMSO alone (1.2 or 0.5%) was also prepared. The growth curve at 37 °C of each *E. coli* culture was obtained by measuring the optical density at 600 nm (OD600) as a function of time using a UV-Vis spectrophotometer.

The synthesis of the manganese complexes was carried out using procedures adapted from previously published works.[35-37] Complexes were kept under darkness at all times during reaction, work up and storage. The tetrazole ligand (1.1 eq.) and triethylamine (3.0 eq.) were added to a 12 mL ethanol/water mixture (3:1 v/v). The mixture was stirred at room temperature for 15 minutes, followed by the addition of *fac*-Mn(diim)$(CO)_3$Br (1.0 eq.). The mixture was then heated at reflux for 4 hours. The resulting yellow solution was reduced in vacuo and 20 mL of dichloromethane were added. The organic phase was collected and washed with water (3 x 20 mL). The organic phase was then dried over anhydrous magnesium sulfate and filtered. The solvent was reduced to few mL, filtered through a 0.2 μm PTFE membrane, and then diethyl ether was added to cause the precipitation of the pure complex as a yellow solid. The solid was filtered and washed with diethyl ether.

fac-Mn(phen)$(CO)_3$**1**

Yield 60 mg (90%). Elemental analysis for $C_{22}H_{13}MnN_6O_3$: calculated C 56.90, H 2.82, N 18.10; found C 56.68, H 2.55, N 17.83. ν_{max} (ATR)/cm^{-1}: 2035 (s) (CO), 1939 (s) (2 x CO). ^{1}H NMR (δ, ppm, Acetone-d_6): 9.73 (2H, dd, $^3J_{H\text{-}H}$ = 4.8 Hz, $^4J_{H\text{-}H}$ = 1.2 Hz, H_4), 8.84 (2H, dd, $^3J_{H\text{-}H}$ = 8.4 Hz, $^4J_{H\text{-}H}$ = 1.2 Hz, H_2), 8.23 (2H, s, H_1), 8.14 (2H, dd, $^3J_{H\text{-}H}$ = 8.4 Hz, $^3J_{H\text{-}H}$ = 4.8 Hz, H_3), 7.68-7.66 (2H, m, H_5), 7.25-7.16 (3H, m, H_6). ^{13}C NMR (δ, ppm, Acetone-d_6): 164.00, 155.22, 148.00, 139.07, 131.81, 130.79, 129.02, 128.60, 128.06, 126.71, 126.55. Crystals suitable for X-ray analysis were grown via evaporation of a solution of dichloromethane containing the complex.

fac-Mn(phen)$(CO)_3$**2**

Yield 42 mg (74 %). Elemental analysis for $C_{21}H_{12}MnN_7O_3$: calculated C 54.20, H 2.60, N 21.07; found C 53.87, H 2.23, N 20.66. ν_{max} (ATR)/cm^{-1}: 2036 (s) (CO), 1941 (s) (2 x CO). ^{1}H NMR (δ, ppm, Acetone-d_6): 9.74 (2H, dd, $^3J_{H\text{-}H}$ = 4.8 Hz, $^4J_{H\text{-}H}$ = 1.2 Hz, H_4), 8.85 (2H, dd, $^3J_{H\text{-}H}$ = 8.4 Hz, $^4J_{H\text{-}H}$ = 1.2 Hz, H_2), 8.79 (1H, s, H_5), 8.39 (1H, d, $^3J_{H\text{-}H}$ = 4.4 Hz, H_7), 8.24 (2H, s, H_1), 8.14 (2H, dd, $^3J_{H\text{-}H}$ = 8.4 Hz, $^3J_{H\text{-}H}$ = 4.8 Hz, H_3), 7.94 (1H, dd, $^3J_{H\text{-}H}$ = 6.4 Hz, $^4J_{H\text{-}H}$ = 1.6 Hz, H_9), 7.23 (1H, dd, $^3J_{H\text{-}H}$ = 8.0 Hz, $^3J_{H\text{-}H}$ = 4.8 Hz, H_8). ^{13}C NMR (δ, ppm, Acetone-d_6): 161.79, 155.28, 149.87, 148.02, 147.96, 139.15, 133.30, 130.82, 128.09, 127.39, 126.77, 124.16. Crystals suitable for X-ray analysis were grown via vapour diffusion of petroleum spirits (40-60 °C) into a solution of dichloromethane containing the complex.

fac-Mn(phen)$(CO)_3$**3**

Yield 36 mg (66 %). Elemental analysis for $C_{21}H_{12}MnN_7O_3$: calculated C 54.20, H 2.60, N 21.07; found C 54.06, H 2.34, N 20.86. ν_{max} (ATR)/cm^{-1}: 2036 (s) (CO), 1941 (s) (2 x CO). ^{1}H NMR (δ, ppm, Acetone-d_6): 9.74 (2H, dd, $^3J_{H\text{-}H}$ = 5.2 Hz, $^4J_{H\text{-}H}$ = 1.2 Hz, H_4), 8.86 (2H, dd, $^3J_{H\text{-}H}$ = 8.4 Hz, $^4J_{H\text{-}H}$ = 1.2 Hz, H_2), 8.44 (2H, d, $^3J_{H\text{-}H}$ = 4.8 Hz, H_6), 8.24 (2H, s, H_1), 8.14 (2H, dd, $^3J_{H\text{-}H}$ = 8.4 Hz, $^3J_{H\text{-}H}$ = 5.2 Hz, H_3), 7.54 (2H, d, $^3J_{H\text{-}H}$ = 5.2 Hz, H_5). ^{13}C NMR (δ, ppm, Acetone-d_6): 162.29, 155.29, 151.10, 147.98, 139.18, 138.49, 130.83, 128.10, 126.78, 120.77. Crystals suitable for X-ray analysis were grown via vapour diffusion of petroleum spirits (40-60 °C) into a solution of dichloromethane containing the complex.

fac-Mn(phen)$(CO)_3$**4**

Yield 40 mg (63 %). Elemental analysis for $C_{23}H_{12}MnN_7O_3$: calculated C 56.45, H 2.47, N 20.04; found C 56.63, H 2.32, N 20.05. ν_{max} (ATR)/cm^{-1}: 2036 (s) (CO), 1942 (s) (2 x CO). ^{1}H NMR (δ, ppm, Acetone-d_6): 9.74 (2H, dd, $^3J_{H\text{-}H}$ = 5.2 Hz, $^4J_{H\text{-}H}$ = 0.8 Hz, H_4), 8.86 (2H, dd, $^3J_{H\text{-}H}$ = 8.4 Hz, $^4J_{H\text{-}H}$ = 0.8 Hz H_2), 8.24 (2H, s, H_1), 8.14 (2H, dd, $^3J_{H\text{-}H}$ = 8.0 Hz, $^3J_{H\text{-}H}$ = 1.2 Hz, H_3), 7.84 (2H, d, $^3J_{H\text{-}H}$ = 8.4 Hz, H_6) 7.65 (2H, d, $^3J_{H\text{-}H}$ = 8.4 Hz, H_5). ^{13}C NMR (δ, ppm, Acetone-d_6): 162.82, 155.31, 147.96, 139.19, 135.80, 133.16, 130.83, 128.11, 127.03, 126.80, 119.37, 111.96. Crystals suitable for X-ray analysis were grown via vapour diffusion of petroleum spirits (40-60 °C) into a solution of dichloromethane containing the complex.

fac-Mn(phen)$(CO)_3$**5**

Yield 46 mg (39%). Elemental analysis for $C_{23}H_{13}MnN_6O_4$: calculated C 56.11, H 2.66, N 17.07; found C 55.77, H 2.47, N 16.92. ν_{max} (ATR)/cm^{-1}: 2036 (s) (CO), 1942 (s) (2 x CO). ^{1}H NMR (δ, ppm, Acetone-d_6): 9.96 (1H, s, H_7) 9.75 (2H, dd, $^3J_{H\text{-}H}$ = 4.8 Hz, $^4J_{H\text{-}H}$ = 1.2 Hz, H_4), 8.86 (2H, dd, $^3J_{H\text{-}H}$ = 8.4 Hz, $^4J_{H\text{-}H}$ = 1.2 Hz, H_2), 8.24 (2H, s, H_1), 8.15 (2H, dd, $^3J_{H\text{-}H}$ = 8.4 Hz, $^3J_{H\text{-}H}$ = 5.2 Hz, H_3), 7.89-7.87 (2H, m, H_6'), 7.81-7.79 (2H, m, H_5). ^{13}C NMR (δ, ppm, Acetone-d_6): 192.36, 163.26, 155.30, 148.00, 139.16, 137.11, 136.96, 130.84, 130.51, 128.10, 126.89, 126.78. Crystals suitable for X-ray analysis were grown via vapour diffusion of ether into a solution of dichloromethane containing the complex.

fac-Mn(batho)$(CO)_3$**1**

Yield 52 mg (79%). Elemental analysis for $C_{36}H_{25}MnN_6O_3$: C 67.08, H 3.91, N 13.04; Found C 66.80, H 3.70, N 13.04. ν_{max} (ATR)/cm^{-1}: 2030 (s) (CO), 1932 (s) (2 x CO). ^{1}H NMR (δ, ppm, Acetone-d_6): 7.99 (2H, s, H_1'), 7.88 (2H, s, H_5'), 7.74 - 7.71 (2H, m, H_7'), 7.65 - 7.60 (10H, m, $H_{2,3,4}$'), 7.28 – 7.21 (3H, m, $H_{8,9}$') 3.55 (6H, s, H_6'). ^{13}C NMR (δ, ppm, DMSO-d_6): 164.09, 162.54, 149.35, 147.85, 135.49, 129.70, 129.61, 129.48, 129.00, 128.53, 128.29, 127.14, 125.41, 125.35, 123.72, 29.08.

fac-Mn(batho)$(CO)_3$**2**

Yield 35 mg (63%). Elemental analysis for $C_{35}H_{24}MnN_7O_3 0.2CH_2Cl_2$: C 63.81, H 3.71, N 14.80; Found C 64.03, H 3.50, N 14.79. ν_{max} (ATR)/cm^{-1}: 2031 (s) (CO), 1934 (s) (2 x CO). (δ, ppm, Acetone-d_6): 8.88 (1H, d, $^4J_{H\text{-}H}$ = 1.2 Hz, H_7'), 8.43 (1H, dd, $^3J_{H\text{-}H}$ = 4.8 Hz, $^4J_{H\text{-}H}$ = 1.6 Hz, H_9') 8.01-7.98 (3H, m, $H_{1,11}$'), 7.89 (2H, s, H_5'), 7.65 - 7.59 (10H, m, $H_{2,3,4}$'), 7.27 (1H, dd, $^3J_{H\text{-}H}$ = 8.4 Hz, $^3J_{H\text{-}H}$ = 4.8 Hz, H_{10}'), 3.56 (6H, s, H_6'). ^{13}C

NMR (δ, ppm, DMSO-d_6): 164.15, 160.35, 149.38, 147.82, 147.63, 146.45, 135.47, 132.63, 129.60, 129.49, 128.99, 128.69, 127.20, 125.47, 125.36, 123.73, 29.11.

fac-Mn(batho)$(CO)_3$**3**

Yield 37 mg (64%). Elemental analysis for $C_{35}H_{24}MnN_7O_3$: C 65.11, H 3.75, N 15.19; Found C 65.17, H 3.56, N 14.95. ν_{max} (ATR)/cm^{-1}: 2031 (s) (CO), 1934 (s) (2 x CO). ^{1}H NMR (δ, ppm, Acetone-d_6): 8.48 (2H, d, J = 3.6 Hz, $H_{8'}$), 8.00 (2H, s, $H_{1'}$), 7.89 (2H, s, $H_{5'}$), 7.65 - 7.59 (12H, m, $H_{2,3,4,6'}$), 3.55 (6H, s, $H_{6'}$). ^{13}C NMR (δ, ppm, DMSO-d6): 164.19, 160.88, 150.21, 149.44, 147.81, 136.50, 135.47, 129.63, 129.53, 129.03, 127.23, 125.38, 123.77, 119.69, 29.12.

fac-Mn(batho)$(CO)_3$**4**

Yield 41 mg (68%). Elemental analysis for $C_{37}H_{24}MnN_7O_3$: C 66.37, H 3.61, N 14.64; Found C 66.36, H 3.52, N 14.42. ν_{max} (ATR)/cm^{-1}: 2031 (s) (CO), 1934 (s) (2 x CO). ^{1}H NMR (δ, ppm, Acetone-d_6): 8.00 (2H, s, $H_{1'}$), 7.90-7.88 (4H, m, $H_{5,7}$), 7.68 (2H, dd, 1H, dd, $^3J_{H-H}$ = 5.6 Hz, $^4J_{H-H}$ = 1.6 Hz, $H_{8'}$), 7.64-7.60 (10H, m, $H_{2,3,4'}$), 3.55 (6H, s, $H_{6'}$). ^{13}C NMR (δ, ppm, DMSO-d_6): 164.19, 161.47, 149.44, 147.80, 135.46, 133.80, 132.80, 129.63, 129.53, 129.04, 127.23, 125.95, 125.38, 123.77, 118.7, 110.67, 29.13.

fac-Mn(batho)$(CO)_3$**5**

Yield 45 mg (73%). Elemental analysis for $C_{37}H_{25}MnN_6O_4$: C 66.07, H 3.75, N 12.49; Found C 66.32, H 3.81, N 12.41. ν_{max} (ATR)/cm^{-1}: 2031 (s) (CO), 1934 (s) (2 x CO). ^{1}H NMR (δ, ppm, Acetone-d_6): 9.98 (1H, s, $H_{9'}$), 8.00 (2H, s, $H_{1'}$), 7.92 (2H, d, $^3J_{H-H}$ = 8.4 Hz, $H_{8'}$), 7.89 (2H, s, $H_{5'}$), 7.83 (2H, d, $^3J_{H-H}$ = 8.4 Hz, $H_{7'}$), 7.65 - 7.61 (10H, m, $H_{2,3,4'}$), 3.56 (6H, s, $H_{6'}$). ^{13}C NMR (δ, ppm, DMSO-d_6): 192.63, 164.24, 161.90, 149.49, 147.91, 135.82, 135.52, 134.99, 130.10, 129.68, 129.59, 129.09, 127.24, 125.91, 125.43, 123.80, 29.17.

X-ray diffraction analysis

All crystals were grown via the diffusion of petroleum spirits into dichloromethane. Crystallographic data for the structures were collected at 100(2) K on either an Oxford Diffraction Xcalibur or Gemini diffractometer. Following Lp, and absorption corrections, and solution by direct methods, the structures were refined against F^2 with full-matrix least squares using the program SHELXL-2014.[46] Anisotropic displacement, parameters were employed for the non-hydrogen atoms. All hydrogen atoms were added at calculated positions and refined by use of a riding model with isotropic displacement parameters based on those of the parent atom. Crystallographic data for the structures reported in this paper can be found in the Supporting Information and have been deposited at the Cambridge Crystallographic Data Centre. CCDC numbers are given below. Copies of the data can be obtained free of charge via https://www.ccdc.cam.ac.uk/structures/, or from the Cambridge Crystallographic Data Centre, 12 Union Road, Cambridge CB2 1EZ, U.KCB21EZ, UK (fax +441223336033; email deposit@ccdc.cam.ac.uk).

Mn(phen)$(CO)_3$**1**, $C_{22}H_{13}MnN_6O_3$, M = 464.32 , 0.168 x 0.145 x 0.102 mm^3, triclinic, space group $P\bar{1}$, a = 9.2137(4), b = 9.3093(5), c = 12.8795(7) Å, α = 106.306(4), β = 96.016(4), γ = 109.134(4)°, V = 977.82(9) $Å^3$, Z = 2, D_c = 1.577 g/cm^3, μ = 0.715 mm^{-1}. λ = 0.71073 Å, T = 100(2) K, $2\theta_{max}$ = 65.2°, 12385 reflections collected, 6444 unique (R_{int} = 0.0337). Final *GooF* = 1.000, *R1* = 0.0431, *wR2* = 0.0918, R indices based on 5129 reflections with $I > 2\sigma(I)$, $|\Delta\rho|_{max}$= 0.50(8) e $Å^{-3}$, 289 parameters, 0 restraints. CCDC number 1938962.

Mn(phen)$(CO)_3$**2**, $C_{21}H_{12}MnN_7O_3$, M = 465.32, 0.224 x 0.188 x 0.143 mm^3, triclinic, space group $P\bar{1}$, a = 9.1185(3), b = 9.2141(3), c = 12.7940(4) Å, α = 95.906(3), β = 104.413(3), γ = 108.911(3)°, V = 964.94(6) $Å^3$, Z = 2, D_c = 1.601 g/cm^3, μ = 0.726 mm^{-1}. λ = 0.71073 Å, T = 100(2) K, $2\theta_{max}$ = 64.6°, 20219 reflections collected, 6405 unique (R_{int} = 0.0326). Final *GooF* = 1.066, *R1* = 0.0386, *wR2* = 0.0951, R indices based on 5475 reflections with $I > 2\sigma(I)$, $|\Delta\rho|_{max}$= 0.62(8) e $Å^{-3}$, 289 parameters, 0 restraints. CCDC number 1938963

Mn(phen)$(CO)_3$**3**, $C_{21}H_{12}MnN_7O_3$, M = 465.32, 0.183 x 0.134 x 0.062 mm^3, monoclinic, space group *C2/c*, a = 20.0296(8), b = 8.2582(3), c = 25.1697(14) Å, β = 107.279(5) °, V = 3975.4(3) $Å^3$, Z = 8, D_c = 1.555 g/cm^3, μ = 5.759 mm^{-1}. λ = 1.54184 Å, T = 100(2) K, $2\theta_{max}$ = 134.6°, 15582 reflections collected, 3530 unique (R_{int} = 0.0598). Final *GooF* = 1.055, *R1* = 0.0468, *wR2* = 0.1267, R indices based on 3109 reflections with $I > 2\sigma(I)$, $|\Delta\rho|_{max}$= 0.51(7) e $Å^{-3}$, 289 parameters, 0 restraints. CCDC number 1938964.

Mn(phen)$(CO)_3$**4**, $C_{23}H_{12}MnN_7O_{3.}3/4(CH_2Cl_2)$, M = 553.03, 0.646 x 0.133 x 0.042 mm^3, monoclinic, space group *C2/c*, a = 22.4035(6), b = 17.2137(4), c = 12.7060(2) Å, β = 91.659(2) °, V = 4897.98(19) $Å^3$, Z = 8, D_c = 1.500 g/cm^3, μ = 0.744 mm^{-1}. λ = 0.71073 Å, T = 100(2) K, $2\theta_{max}$ = 64.2°, 27473 reflections collected, 8088 unique (R_{int} = 0.0355). Final *GooF* = 1.055, *R1* = 0.0605, *wR2* = 0.1474, R indices based on 6603 reflections with $I > 2\sigma(I)$, $|\Delta\rho|_{max}$= 1.36(9) e $Å^{-3}$, 363 parameters, 16 restraints. CCDC number 1938965.

Mn(phen)$(CO)_3$**5**, $C_{23}H_{13}MnN_6O_4$, M = 492.33, 0.436 x 0.356 x 0.093 mm^3, monoclinic, space group $P2_1/n$, a = 9.4795(2), b = 10.9716(2), c = 20.6393(4) Å, β = 97.321(2) °, V = 2129.10(7) $Å^3$, Z = 4, D_c = 1.536 g/cm^3, μ = 0.665 mm^{-1}. λ = 0.71073 Å, T = 100(2) K, $2\theta_{max}$ = 65.4°, 45622 reflections collected, 7422 unique (R_{int} = 0.0330). Final *GooF* = 1.001, *R1* = 0.0364, *wR2* = 0.0977, R indices based on 6273 reflections with $I > 2\sigma(I)$, $|\Delta\rho|_{max}$= 0.45(7) e $Å^{-3}$, 307 parameters, 0 restraints. CCDC number 1938966.

References

[1] R. Motterlini, B. E. Mann, R. Foresti, *Expert Opin. Investig. Drugs.* **2005**, *14*, 1305-1318.

[2] T. R. Johnson, B. E. Mann, J. E. Clark, R. Foresti, C. J. Green, R. Motterlini, *Angew. Chem. Int. Ed.* **2003**, *42*, 3722-3729.

[3] B. E. Mann, *Organometallics* **2012**, *31*, 5728-5735.

[4] S. W. Ryter, J. Alam, A. M. K. Choi, *Physiol. Rev.* **2006**, *86*, 583-650.

[5] K. Schmidt, M. Jung, R. Keilitz, B. Schnurr, R. Gust, *Inorg. Chim. Acta* **2000**, *306*, 6-16.

[6] R. Motterlini, B. Haas, R. Foresti, *Med. Gas Res.* **2012**, *2*, 28-28.

[7] F. Amersi, X. D. Shen, D. Anselmo, J. Melinek, S. Iyer, D. J. Southard, M. Katori, H. D. Volk, R. W. Busuttil, R. Buelow, J. W. Kupiec-Weglinski, *Hepatology* **2002**, *35*, 815-823.

[8] K. Sato, J. Balla, L. Otterbein, R. N. Smith, S. Brouard, Y. Lin, E. Csizmadia, J. Sevigny, S. C. Robson, G. Vercellotti, A. M. Choi, F. H. Bach, M. P. Soares, *J. Immunol.* **2001**, *166*, 4185.

[9] E. O. Leo, H. B. Fritz, A. Jawed, S. Miguel, L. Hong Tao, W. Mark, J. D. Roger, A. F. Richard, M. K. C. Augustine, *Nat. Med.* **2000**, *6*, 422.

[10] S. P. Gaine, G. Booth, L. Otterbein, N. A. Flavahan, A. M. K. Choi, C. M. Wiener, *J. Vasc. Res.* **1999**, *36*, 114-119.

[11] M. A. Gentile, *Respir. Care.* **2011**, *56*, 1341-1357.

[12] J. Boczkowski, J. J. Poderoso, R. Motterlini, *Trends Biochem. Sci.* **2006**, *31*, 614-621.
[13] S. García-Gallego, G. J. L. Bernardes, *Angew. Chem. Int. Ed.* **2014**, *53*, 9712-9721.
[14] R. Motterlini, J. E. Clark, R. Foresti, P. Sarathchandra, B. E. Mann, C. J. Green, *Circ Res* **2002**, *90*, E17-24.
[15] J. Jimenez, I. Chakraborty, S. J. Carrington, P. K. Mascharak, *Dalton Trans.* **2016**, *45*, 13204-13213.
[16] I. Chakraborty, S. J. Carrington, P. K. Mascharak, *Acc. Chem. Res.* **2014**, *47*, 2603-2611.
[17] E. Kottelat, *Inorganics* **2017**, *5*, 24.
[18] P. C. Ford, *Coord. Chem. Rev.* **2018**, *376*, 548-564.
[19] M. A. Wright, J. A. Wright, *Dalton Trans.* **2016**, *45*, 6801-6811.
[20] T. Slanina, P. Ebej, *Photochem. Photobiol. Sci.* **2018**, *17*, 692-710.
[21] R. D. Rimmer, A. E. Pierri, P. C. Ford, *Coord. Chem. Rev.* **2012**, *256*, 1509-1519.
[22] Z. Li, A. E. Pierri, P.-J. Huang, G. Wu, A. V. Iretskii, P. C. Ford, *Inorg. Chem.* **2018**, *57*, 6191-6191.
[23] B. J. Aucott, J. S. Ward, S. G. Andrew, J. Milani, A. C. Whitwood, J. M. Lynam, A. Parkin, I. J. S. Fairlamb, *Inorg. Chem.* **2017**, *56*, 5431.
[24] J. Ward, J. Bray, B. Aucott, C. Wagner, N. Pridmore, A. Whitwood, J. Moir, J. Lynam, I. Fairlamb, *Eur. J. Inorg. Chem.* **2016**, *2016*, 5044-5051.
[25] S. H. C. Askes, G. U. Reddy, R. Wyrwa, S. Bonnet, A. Schiller, *J. Am. Chem. Soc.* **2017**, *139*, 15292.
[26] R. Mede, S. Gläser, B. Suchland, B. Schowtka, M. Mandel, H. Görls, S. Krieck, A. Schiller, M. Westerhausen, *Inorganics* **2017**, *5*, 8.
[27] M. V. Werrett, P. J. Wright, P. V. Simpson, P. Raiteri, B. W. Skelton, S. Stagni, A. G. Buckley, P. J. Rigby, M. Massi, *Dalton Trans.* **2015**, *44*, 20636-20647.
[28] C. A. Bader, R. D. Brooks, Y. S. Ng, A. Sorvina, M. V. Werrett, P. J. Wright, A. G. Anwer, D. A. Brooks, S. Stagni, S. Muzzioli, M. Silberstein, B. W. Skelton, E. M. Goldys, S. E. Plush, T. Shandala, M. Massi, *RSC Adv.* **2014**, *4*, 16345-16351.
[29] N. Akabar, V. Chaturvedi, G. E. Shillito, B. J. Schwehr, K. C. Gordon, G. S. Huff, J. J. Sutton, B. W. Skelton, A. N. Sobolev, S. Stagni, D. J. Nelson, M. Massi, *Dalton Trans.* **2019**, in press, DOI: 10.1039/C9DT02198A.
[30] C. A. Bader, E. A. Carter, A. Safitri, P. V. Simpson, P. Wright, S. Stagni, M. Massi, P. A. Lay, D. A. Brooks, S. E. Plush, *Mol. Biosyst.* **2016**, *12*, 2064-2068.
[31] E. O. John, R. D. Willett, B. Scott, R. L. Kirchmeier, J. n. M. Shreeve, *Inorg. Chem.* **1989**, *28*, 893-897.
[32] J.-M. Lin, B.-S. Huang, Y.-F. Guan, Z.-Q. Liu, D.-Y. Wang, W. Dong, *CrystEngComm* **2009**, *11*, 329.
[33] Y.-B. Lu, M.-S. Wang, W.-W. Zhou, G. Xu, G.-C. Guo, J.-S. Huang, *Inorg. Chem.* **2008**, *47*, 8935-8942.
[34] C. Janiak, T. G. Scharmann, K. W. Brzezinka, P. Reich, *Chem. Ber.* **1995**, *128*, 323-328.
[35] M. V. Werrett, G. S. Huff, S. Muzzioli, V. Fiorini, S. Zacchini, B. W. Skelton, A. Maggiore, J. M. Malicka, M. Cocchi, K. C. Gordon, S. Stagni, M. Massi, *Dalton Trans.* **2015**, *44*, 8379-8393.
[36] M. V. Werrett, S. Muzzioli, P. J. Wright, A. Palazzi, P. Raiteri, S. Zacchini, M. Massi, S. Stagni, *Inorg. Chem.* **2014**, *53*, 229-243.
[37] M. V. Werrett, D. Chartrand, J. D. Gale, G. S. Hanan, J. G. Maclellan, M. Massi, S. Muzzioli, P. Raiteri, B. W. Skelton, M. Silberstein, S. Stagni, *Inorg. Chem.* **2011**, *50*, 1229-1241.
[38] J. Jimenez, I. Chakraborty, P. K. Mascharak, *Eur. J. Inorg. Chem.* **2015**, 5021-5026.
[39] U. Schatzschneider*, Vol. 2010*, Photoactivated Biological Activity of Transition-Metal Complexes, **2010**, pp. 1451-1467.
[40] J. Betts, C. Nagel, U. Schatzschneider, R. Poole, R. M. La Ragione, *PLoS ONE* **2017**, *12*, e0186359.
[41] C. Nagel, S. McLean, R. K. Poole, H. Braunschweig, T. Kramer, U. Schatzschneider, *Dalton Trans.* **2014**, *43*, 9986-9997.
[42] J. S. Ward, R. Morgan, J. M. Lynam, I. J. S. Fairlamb, J. W. B. Moir, *MedChemComm* **2017**, *8*, 346-352.
[43] N. Rana, H. E. Jesse, M. Tinajero-Trejo, J. A. Butler, J. D. Tarlit, M. L. von und zur Muhlen, C. Nagel, U. Schatzschneider, R. K. Poole, *Microbiology* **2017**, *163*, 1477-1489.
[44] P. V. Simpson, C. Nagel, H. Bruhn, U. Schatzschneider, *Organometallics* **2015**, *34*, 3809-3815.
[45] P. Sharrock, *Can. J. Microbio.l* **1985**, *31*, 367-370.
[46] G. M. Sheldrick, *Acta Cryst. C.* **2015**, *71*, 3-8.

Graphical Abstract

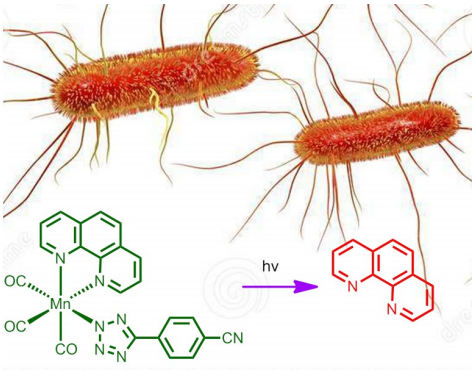

Tricarbonyl manganese(I) diimine tetrazolato complexes are photochemically active, undergoing ligand release upon irradiation to the lower metal-to-ligand charge transfer manifold. The liberated diimine ligands can be exploited to inhibit *Escherichia Coli* growth.

Keywords: bacteria, manganese, photochemistry, tetrazoles, tricarbonyl.